

# Application of GRA and TOPSIS Optimization Techniques in GTA Welding of 15CDV6 Aerospace Material

L. Srinivasan<sup>1</sup> · Khan Mohammad Chand<sup>2</sup> · T. Deepan Bharathi Kannan<sup>1</sup> · P. Sathiya<sup>1</sup> · S. Biju<sup>3</sup>

Received: 24 February 2017 / Accepted: 13 June 2017 / Published online: 30 June 2017  
© The Indian Institute of Metals - IIM 2017

**Abstract** In this article, an attempt was made to optimize the welding parameters of gas tungsten arc welding of 15CDV6 steel. Experiments based on Taguchi's L9 orthogonal array were carried out in this research paper. The input parameters such as current, voltage, travel speed were considered for joining 15CDV6 plates of thickness 3.7 mm. Aftermath, the welds were subjected to post weld heat treatment. The performance characteristics such as bead width, reinforcement, tensile strength, hardness and depth of penetration of the welds were also measured. Grey relational analysis (GRA) and technique for order preference by similarity to ideal solution method (TOPSIS) were used for identifying the optimised input parameters. Analysis of variance was used to identify the influence of each individual parameter on the multi-objective function. The metallurgical characterisations of the optimised weld were compared with the microstructures obtained using optical microscope. It was made clear that both GRA and TOPSIS produced different set of optimized parameters. But on experimentation, it was found that optimized parameters obtained from TOPSIS produced weld with better properties. At the initial stage, the base metal reflected inferior properties to weldments but there was a significant improvement in the properties of base metal after post weld heat treatment.

**Keywords** 15CDV6 · GTAW process · Microstructure · GRA · TOPSIS · ANOVA

## 1 Introduction

Earlier attempts to develop AFNOR 15CDV6 steel was launched in France. The letters C, D and V denotes carbon, molybdenum and vanadium. As the alloying elements remain less than 5% in proportion by weight, the steel fits into the category of low alloy steel [1, 2]. 15CDV6 is a low carbon bainitic steel with high strength, toughness and ductility which finds growing popularity in the fields of aerospace, defence and power generation industries and it is specially used in making rocket motor hardware in the Indian Space Program [3, 4]. Despite the other uses, 15CDV6 steel finds its application in making parts of jet engines, nuclear reactor, pressure vessels, and rocket motor casings [5]. The microstructure of 15CDV6 steel in hardened and tempered condition is composed of predominantly lower bainite and a small proportion of lath martensite. [2]. 15CDV6 steel acquires its strength from hardening at  $975 \pm 5$  °C followed by forced air quenching and tempering at  $640 \pm 5$  °C. Generally, hardening and tempering enables in increasing the strength of steel. The fine dispersion of alloy carbides has a major impact in strengthening of the steel. By increasing the tempering temperature and holding time, there is a decrease in the strength and hardness, and at the same time increases the ductility of the material [3]. The properties of steel has been increased through electro slag refining (ESR) process, resulting in sharp increase in ductility and toughness but rather gradual increase in strength [6]. In order to increase the strength of the steel, the proportion of martensite has to be increased to 0.75 in a mixed microstructure of

✉ P. Sathiya  
psathiya@nitt.edu

<sup>1</sup> Department of Production Engineering, National Institute of Technology, Trichy, Tamilnadu 620015, India

<sup>2</sup> Department of Mechanical Engineering, K. Ramakrishnan College of Engineering, Trichy, Tamilnadu 621112, India

<sup>3</sup> Vikram Sarabhai Space Centre, ISRO, Thiruvananthapuram, Kerala 695022, India

martensite and bainite. This can also be achieved by addition of alloying elements which slows down the bainite reaction. Hence increasing the content of chromium from 1.5 to 4%, increases the strength of the steel, thus helping in the retardation of bainite reaction [4, 7].

The other way to increase the strength is by raising heterogeneous nucleation during solidification by inoculation technique which refines the grain size thereby enhancing the strength [8]. Any manufacturing capability need to be proved through suitable application of any material. In this case, welding capability is demonstrated through the 15CDV6, the most used metal joining process. 15CDV6 has good weldability and ease of fabrication [3, 4]. Chandrasekhar et al. [9] studied electron beam welding and TIG welding, the commonly used welding processes for fabrication using 15CDV6 steel. Ramesh et al. [3] in their work, depicted the parent materials with heat treatment followed by laser beam welding and studied the microstructural evaluation in different regions of the welds. Optimization of the welding process parameters depends upon the ability to measure and control the process variables involved in the welding process. The major contributing parameters of gas tungsten arc welding (GTAW) process are current, voltage, travel speed and gas flow rate. Among the various optimization techniques, grey relational analysis (GRA) and TOPSIS have earned the market due to their multi criteria decision making approaches. This means that GRA and TOPSIS are simple and effective tools to solve the multiple objective problems. GRA and TOPSIS are techniques of multi objective optimization which solves by converting the multi objective function into a single objective function. Deepan Bharathi Kannan et al. [10] in their work successfully used GRA technique in finding the optimized welding parameters in Laser joining of NiTiInol shape memory alloy. Seyed Mostafa Mirhedayatian et al. [11] used a combination of data envelopment analysis (DEA) and TOPSIS for the selection of welding process parameters for repairing nodular cast iron engine block. The combination of these two techniques not only enables in optimizing the welding parameters but also extends to varied fields of manufacturing. Muthuramalingam and Mohan [12] successfully used GRA for Multi objective optimization of electrical process parameters in electrical discharge machining. Durairaj et al. [13] successfully used Grey Relational Theory to optimize the cutting parameters in wire EDM for SS304. Lan et al. [14] used TOPSIS in selecting the optimized parameters in CNC turning process.

From literatures, it is understood that welding of 15CDV6 using GTA welding process produces weldments with better properties than the base material which leads to failure at the base material region during tensile testing. In order to homogenize the base metal and weldment region,

heat treatment is mandatory. Hence, the workpiece after welding is to be subjected to heat treatment and Post weld heat treated coupon properties should be further used for analysis.

It is also understood from the literatures that only fewer research has been emphasised on welding of 15CDV6 and no such publications related to optimization of the welding parameters using GRA and TOPSIS techniques exist. Hence, this research puts an effort to weld 15CDV6 using GTA welding process and optimize the welding parameters using GRA and TOPSIS techniques.

## 2 Materials and Methods

The plate with dimensions  $300 \times 150 \times 3.7$  mm was used for welding. The chemical composition of the base metal is given in Table 1 and the mechanical properties in annealed conditions are given in Table 2. 8CD12 filler wire was used in GTAW of 15CDV6 steel. In order to minimize the formation of Vanadium Carbide, the usage of filler wire as Vanadium was barred. The Chemical composition in filler wire is given in Table 1. The specifications for TIG welding process are given in Table 3.

Taguchi provided an efficient method to find the optimal combination of input parameters. This method used the orthogonal array of experiments to reduce the number of experiments. L9 orthogonal array was used in the present work. The levels for the input parameters are given in Table 4.

Table 5 Shows the L9 orthogonal array experimental run along with output responses [bead width (BW), reinforcement (R), tensile strength (TS), hardness (Hv) and depth of penetration (DoP)] measured after post weld heat treatment.

The weld joint configuration is shown Fig. 1.

After welding, the samples were subjected to heat treatment as per heat treatment cycle shown in Table 6. They were sliced to the required size for analyzing. The samples were then etched with Nital (5% nitric acid). Optical microscopy was used to characterize the various regions of weldments. Micro hardness evaluation was carried out at regular intervals (2 mm) across the weldments at a load of 500 g. The test specimens were made by water jet cutting and the mechanical properties were evaluated at room temperature as per ASTM E-8 specification. The heat input was calculated using the following equation

$$\text{Heat input (HI)} = \frac{\eta \times I \times V \times 60}{S} \quad (1)$$

where  $\eta$  = arc efficiency,  $I$  = current in A,  $V$  = voltage in V,  $S$  = travel speed in mm/min.

**Table 1** Chemical composition (wt %) of materials (Nominal)

Material	C	Mn	Si	Mo	V	Cr	P	S	Fe
Base	0.12–0.18	0.8–1.10	0.2	0.80–1.0	0.20–0.30	1.25–1.50	0.02 Max	0.0015 Max	Bal.
Filler	0.1	1.1	0.9	1.0	–	3.0	0.015	0.009	Bal.

**Table 2** Base Material Mechanical Properties (annealed) [15]

Ultimate tensile strength (MPa)	Proof stress (MPa)	Elongation (%)	Hardness (BHN)	Impact energy (kg/cm <sup>2</sup> )
726	486.8	24.6	209–215	5.81

**Table 3** Machine specifications of GTAW power source

Machine	AC, DC pulse TIG
Duty cycle	60/40
Capacity	370 A
Power supply	DCEN
Electrode	Tungsten alloy (2% thoriated tungsten)
Shielding gas	Argon

**Table 4** Welding parameters and their levels

Factor Notation	Parameters	Level 1	Level 2	Level 3
A	Current (A)	80	110	140
B	Voltage (V)	14	16	18
C	Travel speed (mm/min)	25	45	65
D	Gas flow rate (lpm)	7	8	9

### 3 Results and Discussions

#### 3.1 Grey Relational Approach (GRA)

GRA is a multi-objective optimization technique that converts multi response into single objective problem. GRA has been developed by Deng in 1982, to analyze the

uncertainties in systems and relations between systems. The overall performance of experimental trial depends on grey relational grade. The higher grey relational grade attributes to optimal solution.

It can be used to find correlation among sequences with less number of data and also examines several aspects. In this method all the performance characteristics are converted into a single grey relational grade.

Conversion of the various responses into a single grey relational grade is carried out via the following stages.

##### 3.1.1 Stage 1

Grey relational approach has been employed to analyse the obtained results by using signal-to-noise (S/N) ratio. The signal-to-noise (S/N) ratio is a measure of how much useful information is there in a system or process, as a proportion of the entire content. These (S/N) ratios are calculated for all the output responses based on Eqs. (2) and (3). These ratios can be categorized into three types namely: Smaller is Better (SB), Larger is Better (LB) and Nominal is a Better (NB).

In GTAW welding process, in order to achieve increase in the tensile strength, hardness and depth of penetration of the weldments, ‘Larger is Better’ option has been used.

**Table 5** L9 Orthogonal array with input parameters and output responses

Exp. No.	Input parameters				Output responses				
	A (A)	B (V)	C (mm/min)	D (lpm)	BW (mm)	R (mm)	TS (MPa)	Hv	DoP (mm)
1	80	14	25	7	8.87	1.28	977	335.33	4.99
2	80	16	45	8	8.87	1.32	968	326.33	4.99
3	80	18	65	9	10.9	1.21	959	332.33	4.82
4	110	14	45	9	10.04	2.07	995	342.67	5.04
5	110	16	65	7	10.3	1.10	984	323.67	3.64
6	110	18	25	8	9.46	1.24	973	350.67	4.67
7	140	14	65	8	11.8	2.07	981	362.33	4.45
8	140	16	25	9	3	3.00	1200	600.00	9
9	140	18	45	7	12.53	1.89	1008	367.67	4.34

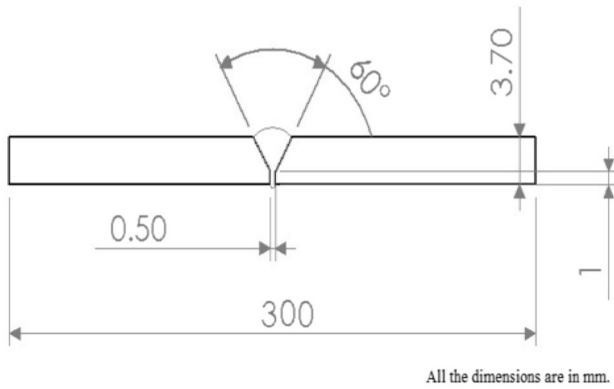


**Fig. 1** Weld joint configuration

Whereas the responses bead width and reinforcement are expected to be of minimum value and hence ‘Smaller is Better’ option has been used for bead width and reinforcement. The values are calculated using the following results.

1. Larger-the-Better

$$S/N \text{ ratio} = -10 \log \left( \frac{1}{n} \sum_{i=1}^n 1/y_{ij}^2 \right) \tag{2}$$

2. Smaller-the-Better

$$S/N \text{ ratio} = -10 \log \left( \frac{1}{n} \sum_{i=1}^n y_{ij}^2 \right) \tag{3}$$

where, n is the number of replications for each experiment,  $Y_{ij}$  are the response values.

3.1.2 Stage 2

The S/N ratios obtained from the Eqs. (2) and (3) have been normalized using the following relations.

1. Larger-the-Better

$$N_i^*(k) = \frac{y_i(k) - \min y_i(k)}{\max y_i(k) - \min y_i(k)} \tag{4}$$

2. Smaller-the-Better

$$N_i^*(k) = \frac{\max y_i(k) - y_i(k)}{\max y_i(k) - \min y_i(k)} \tag{5}$$

where  $i = 1, \dots, m$ ,  $k = 1, 2, 3, \dots, n$ ,  $m =$  no. of trial data,  $n =$  no. of factors,  $y_i(k) =$  original sequence,  $N_i^*(k)$  value after GRG,  $\min y_i(k)$  and  $\max y_i(k)$  are the minimum and maximum value of  $y_i(k)$  respectively.

The Normalized values for the output responses are given in the Table 7.

3.1.3 Stage 3

Grey relation coefficient (GRC) has been calculated to identify the relationship between the ideal and actual normalized experimental results. The computation of GRC is done with the help of equation.

$$\epsilon_i(k) = \frac{\Delta_{\min} + \tau \Delta_{\max}}{\Delta_{oi}(k) + \tau \Delta_{\max}} \tag{6}$$

where  $\epsilon_i(k)$  is the GRC,  $\Delta_{oi}$  is deviation among  $N_o^*(k)$  and  $N_i^*(k)$ ,  $N_o^*(k) =$  ideal (reference) sequence,  $\Delta_{\max} =$  highest value of  $\Delta_{oi}(k)$ ,  $\Delta_{\min} =$  least value of  $\Delta_{oi}(k)$ ,  $\tau$  is assumed to be 0.5 in this case (distinguishing coefficient).

3.1.4 Stage 4

After averaging the grey relational coefficients, the grey relational grade (GRG) has been calculated using the formula:

$$GRG = \left( \frac{1}{m} \right) \sum \epsilon_i(k) \tag{7}$$

where m is the number of response variables.

The high value of grey relational grade indicates the stronger relational degree between ideal sequence and

**Table 6** Heat treatment cycle

Hardening cycle	
Loading temperature	<600 °C
Soaking temperature	975 ± 10 °C
Soaking time	20 min
Quench medium	Forced air
Quench delay (max)	30 s
Tempering cycle	
Loading temperature	<500 °C
Soaking temperature	640 ± 10 °C
Soaking time	30 min
Quench medium	Forced air
Quench delay (max)	30 s

**Table 7** The normalized values for the output responses

Experiment no.	Normalized value				
	BW	R	TS	Hv	DoP
1	0.00	0.17	0.17	0.28	0.97
2	0.00	0.21	0.21	0.06	0.97
3	0.60	0.11	0.11	0.21	0.86
4	0.36	0.75	0.75	0.45	1.00
5	0.43	0.00	0.00	0.00	0.00
6	0.19	0.14	0.14	0.63	0.77
7	0.83	0.75	0.75	0.89	0.62
8	0.87	1.00	1.00	0.61	0.86
9	1.00	0.64	0.64	1.00	0.54

present sequence. The ideal sequence is the best response in the machining process. Higher grey relational grade indicates closeness to the optimal response in the process.

### 3.1.5 Stage 5

The grey relational grade values are then ranked in order. The rank of each trial has been tabulated in Table 8.

From the ranking it is seen that experimental trial 8 shows the highest GRG value in Taguchi’s L9 experimentation. But in order to get the best optimal set of parameters, it is necessary to draw the response table. The response table for the various parameters along with their optimal levels is shown in Table 9. From the response table it can be observed that current was having the maximum range (Max–min) indicating that current is the most influential parameter on the overall objective function followed by shielding gas flow rate, travel speed and voltage.

From the response table it is seen that the optimized set of parameters fits outside Taguchi’s L9 experimentation. It is observed that level 3 in current, level 1 in voltage, level 2 in travel speed and level 3 in gas flow rate form the optimized set of input parameters.

### 3.2 Analysis of Variance (ANOVA)

Analysis of variance (ANOVA) is conducted to determine the significance level of each input parameters affecting the multiple responses of GTAW. ANOVA is constructed using the GRG values from GRA and it is shown in Table 10. The influence of each input parameter thus on the responses is graphically shown in Fig. 2.

Here the error value has become zero, hence pooled error method has been followed to calculate the parameter influence. The two parameters with least sum of squares have been added and it is used as error value and the calculations are done using MINITAB software.

From ANOVA it can be concluded that current is the most influential parameter followed by gas flow rate, travel speed and voltage taken in that order.

### 3.3 Technique for Order Preference by Similarity to Ideal Solution Method (TOPSIS)

TOPSIS is a simple and effective multi criteria decision making tool used in many applications corresponding to sustainable concept selection, location of charging stations, computer networks, site selection for solar farms and process parameter selection in manufacturing etc., TOPSIS is one of the multi criteria decision making methods (MCDM) used to solve multi objective problems. It is based on the concept that the optimized solution should have the shortest distance from the ideal solution and the farthest distance from the negative ideal solution.

The following stages have been employed in this approach:

#### 3.3.1 Stage 1

The data have been normalized using the following relation:

$$R_{ij} = \frac{X_{ij}}{\sum X_{ij}^2} \tag{8}$$

For  $i = 1, \dots, m; j = 1, \dots, n$

#### 3.3.2 Stage 2

Weights are allocated for each criterion considered in optimization. Equal percentage of weights is considered for all the input parameters.

#### 3.3.3 Stage 3

A weighted normalized matrix is built by multiplying each column of the normalized matrix with the respective weights

**Table 8** GRC, GRG and rank for all the output responses for 15CDV6 steel

Experiment no.	GRC					GRG	Rank
	BW	R	TS	Hv	DoP		
1	0.33	0.38	0.38	0.41	0.94	0.49	6
2	0.33	0.39	0.39	0.35	0.94	0.48	7
3	0.55	0.36	0.36	0.39	0.78	0.49	5
4	0.44	0.67	0.67	0.48	1.00	0.65	4
5	0.47	0.33	0.33	0.33	0.33	0.36	9
6	0.38	0.37	0.37	0.57	0.68	0.47	8
7	0.74	0.67	0.67	0.81	0.57	0.69	3
8	0.79	1.00	1.00	0.56	0.78	0.83	1
9	1.00	0.58	0.58	1.00	0.52	0.74	2

**Table 9** Response table for average grey relational grade

	Current (A)	Voltage (B)	Travel speed (C)	Gas flow rate (D)
Level 1	0.49	0.61	0.60	0.53
Level 2	0.49	0.56	0.62	0.55
Level 3	0.75	0.57	0.51	0.66
Max–min	0.26	0.05	0.11	0.13

**Table 10** Analysis of variance (ANOVA) using GRG values in GRA

Sl. no.	Parameters	Degrees of freedom	Sum of squares	Mean square	F value	Percentage contribution (%)
1	Current (A)	2	0.019	0.069	8.40	72.51
2	Voltage (B)	2	0.028	0.002	0.29	2.52
3	Travel speed (C)	2	0.033	0.010	1.18	10.22
4	Gas flow rate (D)	2	0.019	0.014	1.71	14.74
5	Error		0.028	0.008	11.59	
6	Total					100

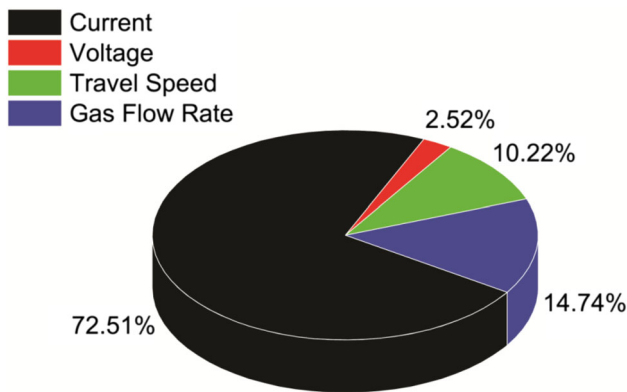


**Fig. 2** The influence of input parameters on the output responses in GRA

$$V_{ij} = W_j R_{ij} \tag{9}$$

Let  $W_j$  be the weights for each input parameter where  $j = 1, \dots, n$  (equal to 0.2).

In order to give equal importance to all the parameters, 20% weightage is chosen for all the output parameters.

The normalized (NM) and weighted normalization matrix (WNM) for the output responses are shown in Table 11.

3.3.4 Stage 4

Ideal and negative ideal solution have been found using the relation given

1. Positive ideal solution.

$$A^+ = \{V_1^+, \dots, V_n^+\},$$

where  $V_j^+ = \{\max(V_{ij}) \text{ if } j \in J; \min(V_{ij}) \text{ if } j \in J'\}$ .

2. Negative Ideal solution.

$$A^- = \{V_1^-, \dots, V_n^-\},$$

where  $V_j^- = \{\min(V_{ij}) \text{ if } j \in J; \max(V_{ij}) \text{ if } j \in J'\}$ .

Positive and negative ideal solutions for all output responses are given in the Table 12.

3.3.5 Stage 5

The separation measure is found out from the positive and negative ideal solution using the relation given as follows:

The separation from the ideal alternative is:

$$S_i^+ = \left[ \sum (V_j^+ - V_{ij})^2 \right]^{1/2} \quad i = 1, \dots, m \tag{10}$$

Similarly, the separation from the negative alternative is:

$$S_i^- = \left[ \sum (V_j^- - V_{ij})^2 \right]^{1/2} \quad i = 1, \dots, m \tag{11}$$

The values for separation measure are tabulated in Table 13.

3.3.6 Stage 6

Relative closeness values of a particular alternative is found using the relation:

$$P_i = \frac{S_i^-}{(S_i^+ + S_i^-)} \quad 0 < P_i < 1 \tag{12}$$

The option with  $P_i$  closest to 1 is selected.

**Table 11** Normalized and weighted normalized values

Exp. no.	BW		R		TS		Hv		DoP	
	NM	WNM	NM	WNM	NM	WNM	NM	WNM	NM	WNM
1	0.28	0.06	0.25	0.05	0.33	0.07	0.33	0.07	0.36	0.07
2	0.28	0.06	0.26	0.05	0.33	0.07	0.32	0.06	0.36	0.07
3	0.34	0.07	0.24	0.05	0.33	0.07	0.32	0.06	0.34	0.07
4	0.32	0.06	0.40	0.08	0.34	0.07	0.33	0.07	0.36	0.07
5	0.32	0.06	0.21	0.04	0.33	0.07	0.31	0.06	0.26	0.05
6	0.30	0.06	0.24	0.05	0.33	0.07	0.34	0.07	0.33	0.07
7	0.37	0.07	0.40	0.08	0.33	0.07	0.35	0.07	0.32	0.06
8	0.38	0.08	0.50	0.10	0.34	0.07	0.34	0.07	0.34	0.07
9	0.39	0.08	0.37	0.07	0.34	0.07	0.36	0.07	0.31	0.06

**Table 12** Positive and negative ideal solution for output responses

	BW	R	TS	Hv	DoP
V <sup>+</sup>	0.05	0.04	0.06	0.07	0.07
V <sup>-</sup>	0.07	0.09	0.06	0.06	0.05

3.3.7 Stage 7

Table 14 shows the relative closeness values of each experimental run. From the list of relative closeness values, it is seen that experimental trial 9 displays the maximum relative closeness value among the nine experiments. Higher relative closeness value indicates that the respective experiment is closer to the ideal value. But in order to get the optimized set of parameters from the TOPSIS methodology, a response table has to be constructed as shown in Table 15. The response table has been formulated using the same logic as used in formulating response table for GRA.

From the response table it is seen that the optimized set of parameters fit outside Taguchi’s L9 experimentation. It is observed that level 1 in current, level 3 in voltage, level 1 in travel speed and level 1 in gas flow rate form the optimized set of input parameters according to TOPSIS.

**Table 13** Separation measure for the various experimental run

Experiment no.	S <sup>+</sup>	S <sup>-</sup>
1	0.01	0.06
2	0.01	0.09
3	0.02	0.09
4	0.04	0.08
5	0.02	0.08
6	0.01	0.09
7	0.04	0.07
8	0.06	0.93
9	0.04	1.94

**Table 14** Relative closeness value

Sl. no.	Relative closeness	Rank
1	0.85	7
2	0.88	8
3	0.84	9
4	0.66	3
5	0.76	6
6	0.90	5
7	0.60	2
8	0.93	4
9	0.97	1

3.4 Analysis of Variance (ANOVA)

ANOVA has been used to find out the significance of various input parameters with respect to the responses. The ANOVA table is shown in Table 16. From the table it is seen that voltage has the most influence on the characteristics of the output followed by travel speed, current and gas flow rate taken in that order. The influence of Input parameters on Output Responses is shown graphically in Fig. 3. The calculations are done based on pooled error method as followed in ANOVA for GRA using MINITAB software.

3.5 Comparison of GRA, TOPSIS Results and Confirmation Test Results

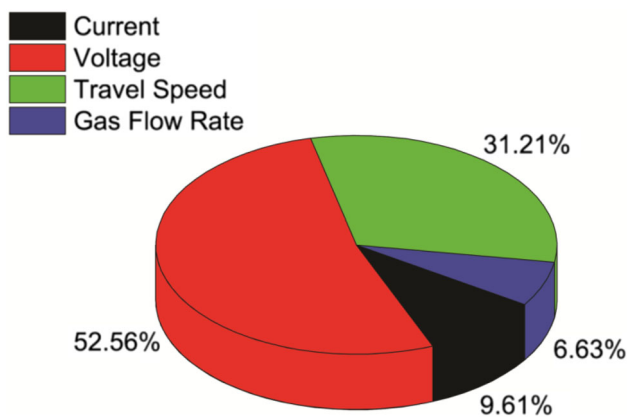
Based on the calculation, it is found that both GRA and TOPSIS yield results outside the Taguchi’s L9 experimentation and also both GRA and TOPSIS yield different set of parameter combinations. In order to compare the results from GRA and TOPSIS and validate the analysis, the predicted closeness value is calculated for both using the following relation.

**Table 15** Response table for average closeness value

	Current (A)	Voltage (B)	Travel speed (C)	Gas flow rate (D)
Level 1	0.86	0.71	0.90	0.87
Level 2	0.78	0.86	0.84	0.80
Level 3	0.84	0.91	0.74	0.82
Max–min	0.09	0.20	0.16	0.07

**Table 16** Analysis of variance (ANOVA) for all the input parameters in TOPSIS

Sl. no.	Parameters	Degrees of freedom	Sum of squares	Mean square	F value	Percentage contribution (%)
1	Current (A)	2	0.012	0.006	0.32	9.61
2	Voltage (B)	2	0.065	0.033	1.78	52.56
3	Travel speed (C)	2	0.039	0.019	1.05	31.21
4	Gas flow rate (D)	2	0.008	0.004	0.22	6.63
5	Error		0.073	0.018	3.38	
6	Total					100

**Fig. 3** The influence of input parameters on output response in TOPSIS

$$\alpha = \alpha_m + \sum (\alpha_n - \alpha_m) \quad (13)$$

$\alpha_m$  = mean of GRG values for the taghuchi's L9 experiments,  $\alpha_n$  = mean grey relational at the optimum level.

The predicted value from Eq. 13 for GRA and TOPSIS are 0.90674 and 1 respectively. The predicted closeness value of TOPSIS is found to be higher than that of GRA. Therefore in this study confirmation test is conducted for the optimized set of parameters obtained from TOPSIS. It is seen that the experimental closeness value is 0.98 which is still a better result than that of the taghuchi's L9 orthogonal array. The results are shown in Table 17.

**Table 17** Optimum process parameters

Sl. no.	Initial	Initial A1B1C1D1	Predicted value A3B1C2D3	Experimental value A3B1C2D3
1	GRG	0.48	1.00	0.98
2	Bead width (BW)	8.87	–	9.10
3	Reinforcement (R)	1.27	–	1.42
4	Tensile Strength (TS)	977	–	1014
5	Hardness (Hv)	335.33	–	365
6	Depth of penetration (DoP)	4.99	–	4.83

### 3.6 Mechanical and Metallurgical Characterization of the Optimized Weld

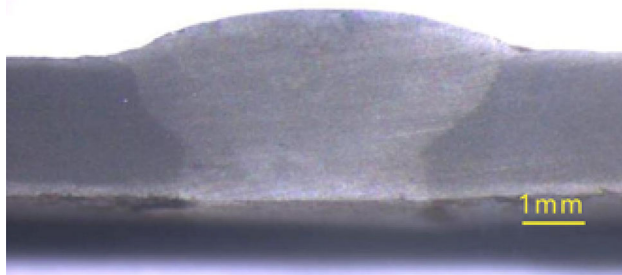
The optimized parameter welding is again carried out and the weld is instantly subjected to heat treatment cycle as done for the L9 experiments and the properties are measured and discussed with the help of microstructure, XRD and fractography.

The macrostructure of the optimized weld is taken with the help of welding expert system (Struers, Austria) with the magnification of 6.25× and is shown in Fig. 4. The bead width, reinforcement, depth of penetration of the optimized weld are 9.10, 1.42 and 4.83 respectively.



The microstructure of the weld, base metal, HAZ of the optimized weld are shown in the Fig. 5. The microstructure of the weld comprise of ferrite, martensite and tempered

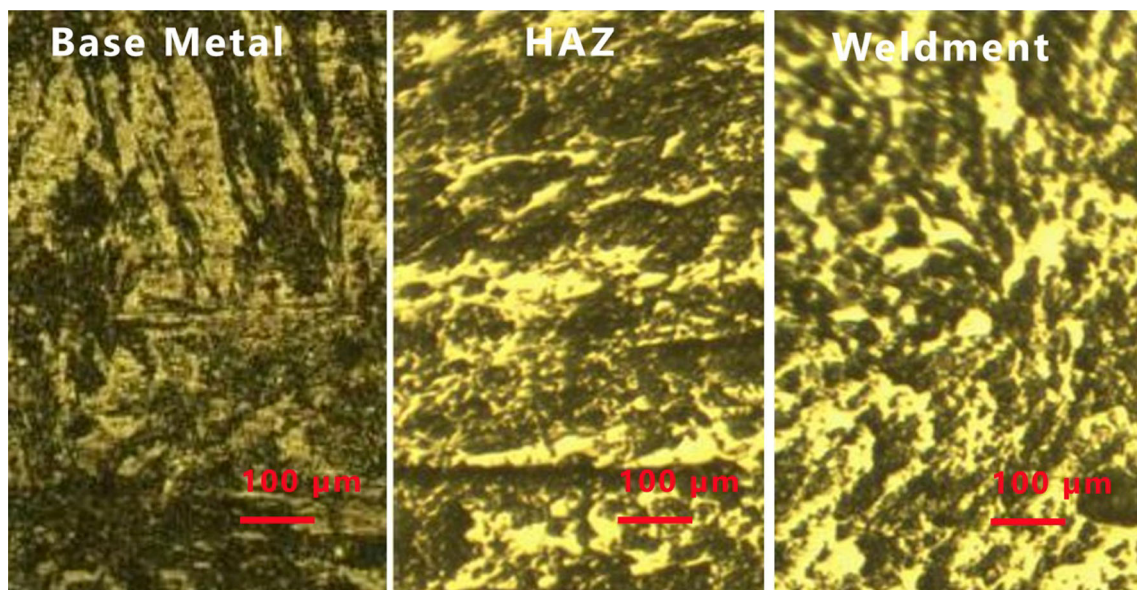
martensite. The bright portion in the microstructure is the ferrite phase and the needle like dark region represents martensite and the irregular shaped dark region represents tempered martensite. In addition to the above said phases, bainite is also found in very small proportions. Comparatively, the weld has finer grain structure leading to better mechanical properties and the base metal microstructure after post weld heat treatment has almost similar properties as that of base metal. There are no defects in all the three zones of the weld.



**Fig. 4** Macrostructure of the weldment obtained with the optimized set of parameters from GRA

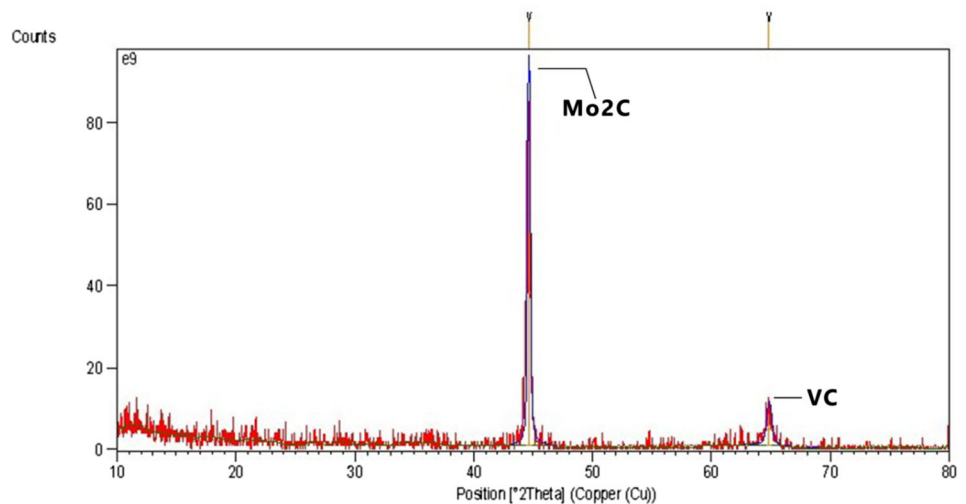
XRD analysis reveals the presence of some inter metallic phases such as  $Mo_2C$  and VC which is shown in Fig. 6.

Microhardness values of the optimised weld are examined along the transverse direction. Microhardness values



**Fig. 5** Microstructure of HAZ and weldment obtained with the optimized set of parameters from GRA

**Fig. 6** XRD for weldment obtained with the optimized set of parameters from GRA



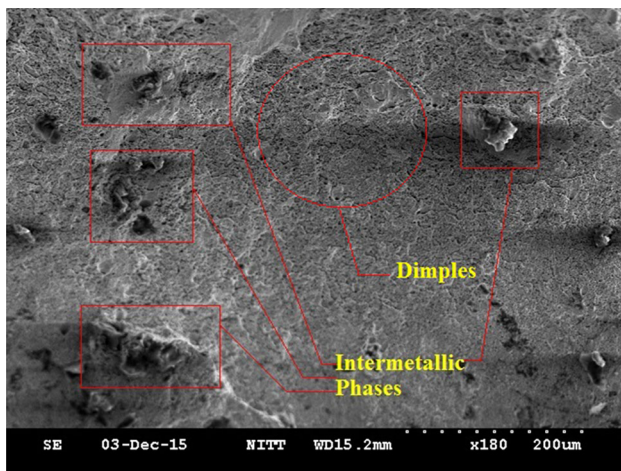


**Fig. 7** SEM image for the weldment obtained with the optimized set of parameters from GRA

are measured at five different points and its average value is taken. It is found that the heat affected zone of the optimised weld region has slightly more microhardness than the weld region. The main reason for this lies on the formation of  $\text{Mo}_2\text{C}$  and VC precipitates during tempering and its distribution is seen more in the heat affected zone. The base metal region microhardness experiences a drastic improvement after heat treatment process. Tensile strength of the optimised weld is measured and it is found that its value is better than the annealed base metal strength. Tensile specimen break in the heat affected zone of the weld region as it have more microhardness than the base metal region. Heat input to the optimised weld has more impact on the tensile strength and it is observed that higher heat input reduces the formation of martensite in the interface of the weld and heat affected zone.

The fractography of the optimized weld tensile tested specimen is shown in the Fig. 7. The fractography reveals the presence of dimples which signifies the ductile mode of failure and also the presence of some inter metallic phases are seen in the fractograph.

The Properties of the base metal after post weld heat treatment are as follows: Ultimate tensile strength—995 MPa, Microhardness—350 Hv. Thus in this work the properties of both weld and base metal after post heat treatment are made almost same.

#### 4 Conclusion

Butt joint were successfully made between 3.7 mm thick 15CDV6 plates using GTA welding process. The input parameters were successfully optimized using GRA and TOPSIS and the following conclusions were drawn.

1. Full penetration was achieved in all the nine experimental runs.
2. Both in GRA and TOPSIS, the optimized set of parameters were found to be outside the L9 experimental run. Since the predicted GRG value in GRA was lower than predicted closeness value in TOPSIS, confirmation test was done based on the TOPSIS optimized parameter combination and confirmation test results were in good agreement with the actual results.
3. The Optimized parameter combinations obtained using TOPSIS were current = 110 A, voltage = 18 V, travel speed = 25 mm/min, gas flow rate = 7 lpm and the corresponding output values were bead width = 9.10 mm, reinforcement = 1.42 mm, tensile strength = 1014 MPa, hardness = 365 Hv, depth of penetration = 4.83 mm.
4. From GRG value, ANOVA indicated that current was the major influencing factor on the overall objective and in the case of ANOVA done with the TOPSIS relative closeness value, voltage was found to be the most influencing factor.
5. After post weld heat treatment, the base metal attained properties similar to that of weldments.

#### References

1. Kumar P, Naveen Bhaskar Y, Mastanaiah P, and Murthy C V S, *Proc Mater Sci* **5** (2014) 2382.
2. Chandra Sekhar M, Srinivasa Rao D, and Dasari Ramesh, *IJRRCME* **1** (2014) 12.
3. Ramesh M V L, Srinivasa Rao P, and Venkateswara Rao V, *Def Sci J* **65** (2015) 339.
4. Bandyopadhyay T R, Rao P K, and Prabhu N, *ISRN Mat Sci* **2012** (2012) 1.
5. Saphthagiri S, Jayathirtha Rao K, Ashok Reddy K, and Sharada Prabhakar C, *IJARF* **2** (2015) 16.
6. Padki G M, Balasubramanian M S N, Gupt K M, and Krishna Rao P, *Ir Mak St Mak* **10** (1983) 180.
7. Young C H, and Bhadeshia H K D H, *Mat Sci Technol* **10** (1994) 209.
8. Campbell J, and Bannister J W, *Met Technol* **2** (1975) 409.
9. Chandrasekhar Neelamegam, Vishnuvardhan Sapineni, Vasudevan Muthukumaran L, and Jayakumar Tamanna, *J Intell Learn Syst Appl* **5** (2013) 39.
10. Deepan Bharathi Kannan T, Pavani Priya T, Ramesh T, and Sathiya P, *Pro Mat Tod* **4** (2017) 1268.
11. Seyed Mostafa Mirhedayatiana, Seyed Ebrahim Vahdat, Mostafa Jafarian Jelodar, and Reza Farzipoor Saen, *Mater Des* **43** (2013) 272.
12. Muthuramalingam T, and Mohan B, *Ind J Eng Mater Sci* **20** (2013) 471.
13. Durairaj M, Sudharsun D, Swamynathan B, *ICNDM* **64** (2013) 868.
14. Lan, *Inf Technol J* **8** (2009) 917.
15. Sinha P P, Murthy M S P, Ghosh B R, and Mittal M C, ISRO-VSSC-TR-36 (1980).